Active Galactic Nuclei – II
X-ray emission and internal structure

AGN X-ray emission

High-energy emission from AGN

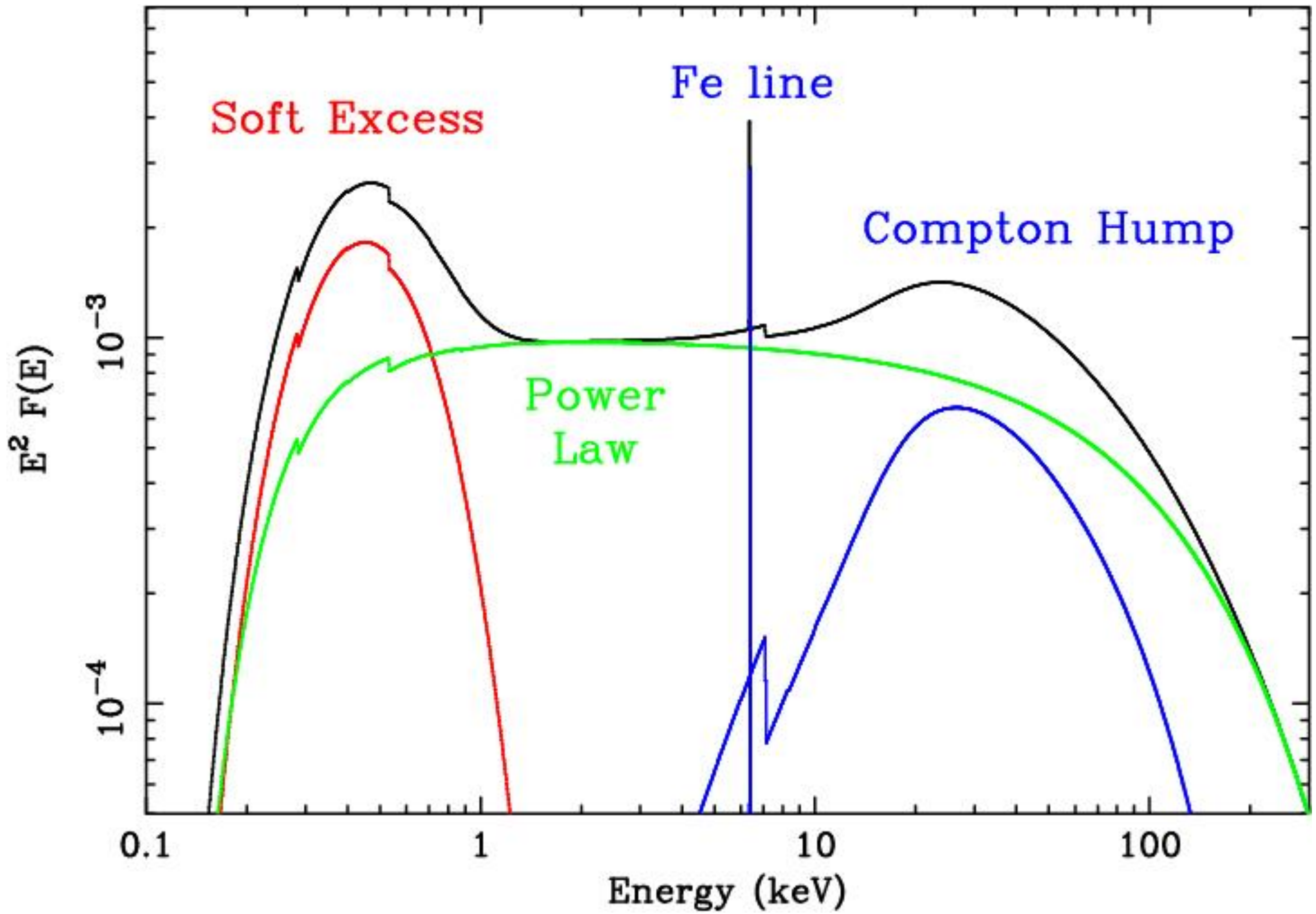

High-energy emission from AGN

Alternative hypotheses to the disc BB emission (more likely related to *warm Comptonicazion*)

if BB, we should see a range of kT in X-rays, which is not observed

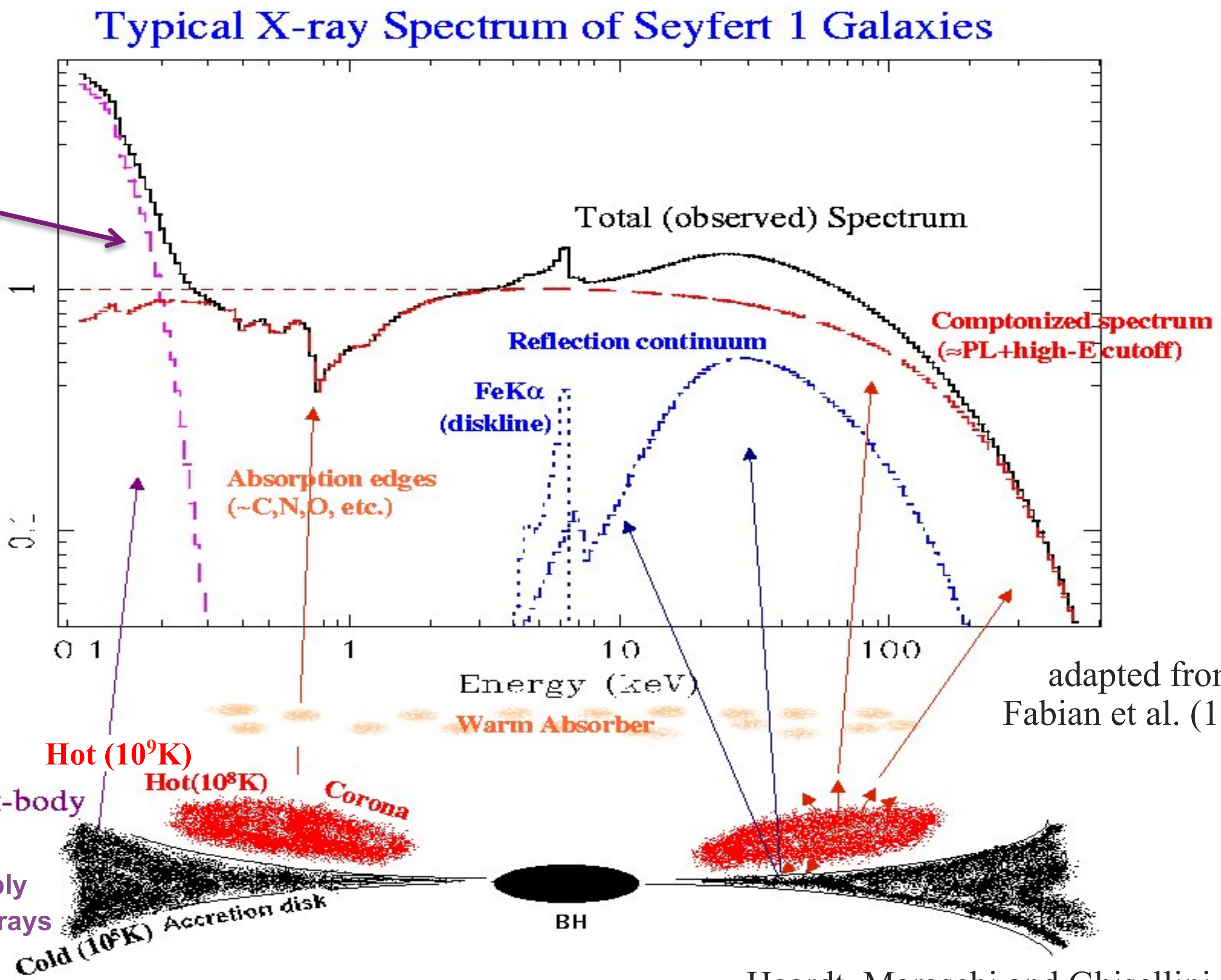

probably not in X-rays

adapted from Fabian et al. (1997)

Haardt, Maraschi and Ghisellini (1994)

High-energy emission from AGN: thermal Comptonization (I)

[I] Primary power-law emission: Comptonization: hot electrons vs. cold photons from the accretion disc (Inverse Compton emission).
The heating mechanism of the corona is largely unknown (magnetic reconnection?)

$E << 4kT_e$: the photon can gain energy in each of the N scatterings event (IC)

$\Delta E/E \approx 4kT_e/m_ec^2$

y=Compton parameter≈
$\approx 4kT_e/m_ec^2 \max(\tau,\tau^2)$

N depending on the optical depth of the electron gas

$$E_f \approx E_i \exp\left(N\frac{4kT_e}{m_ec^2}\right) \approx E_i \exp(y)$$

Reminder: Comptonization

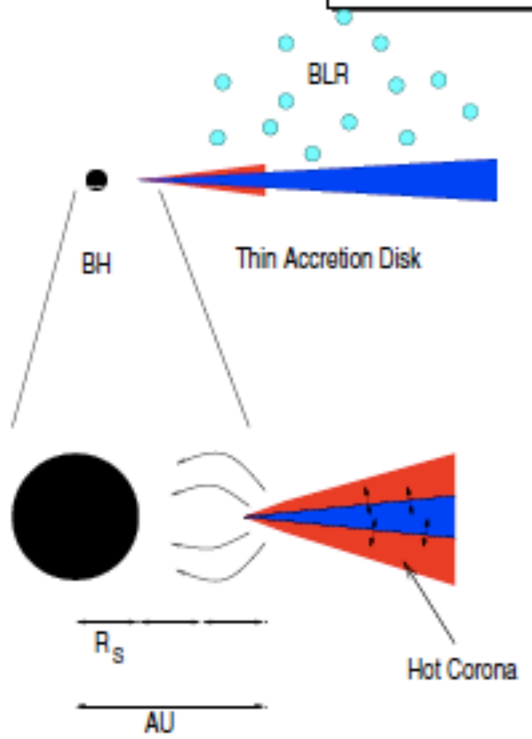

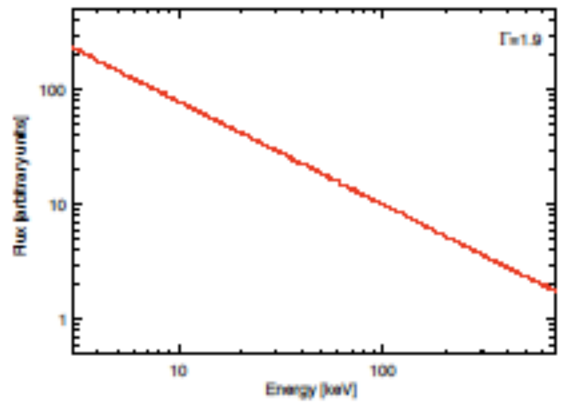

AGN X-Ray Spectrum:

- Comptonization of soft X-rays from accretion disk in hot corona ($T \sim 10^8$ K): power law continuum.

High-energy emission from AGN: thermal Comptonization (II)

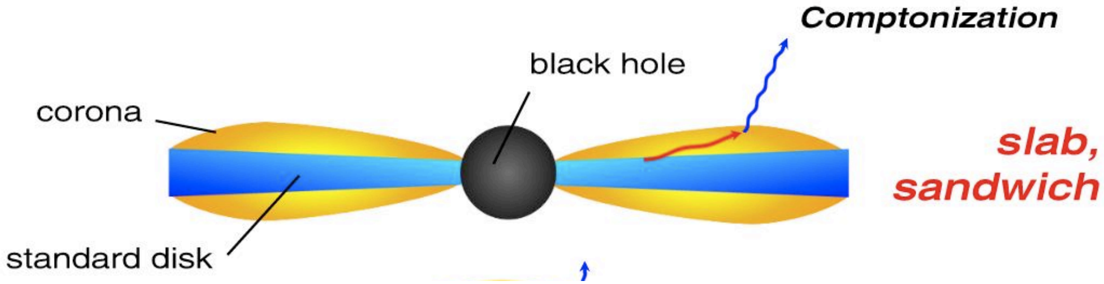

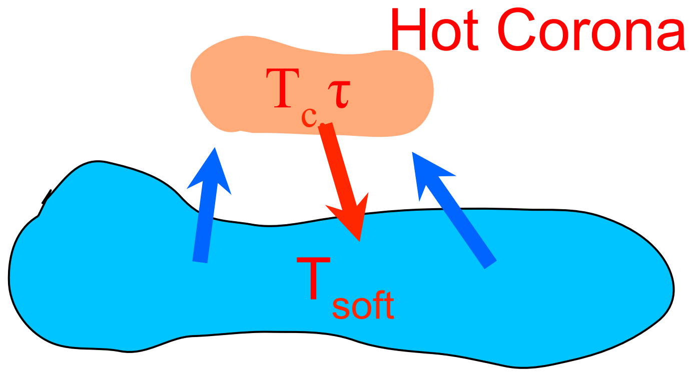

Cold phase (disc)

Thermal Comptonization from thermal electrons plasma with kT and optical depth τ

Structure of the corona still unknown

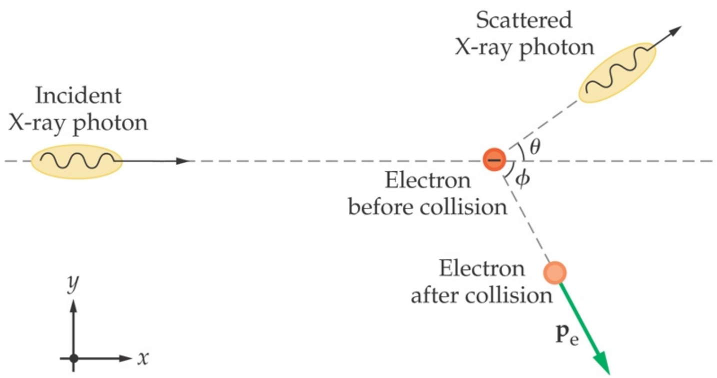

Location of the corona ≈ within tens of Rg from the corona (Chartas+, Kara+, De Marco+), estimated for few AGN thus far

If electron at rest:

$$\Delta E = E' - E \simeq -\frac{E^2}{m_e c^2}(1 - \cos\theta)$$

For non-stationary electron:

$\Delta E < 0 \rightarrow$ Compton

$\Delta E > 0 \rightarrow$ Inverse Compton

High-energy emission from AGN: thermal Comptonization (III)

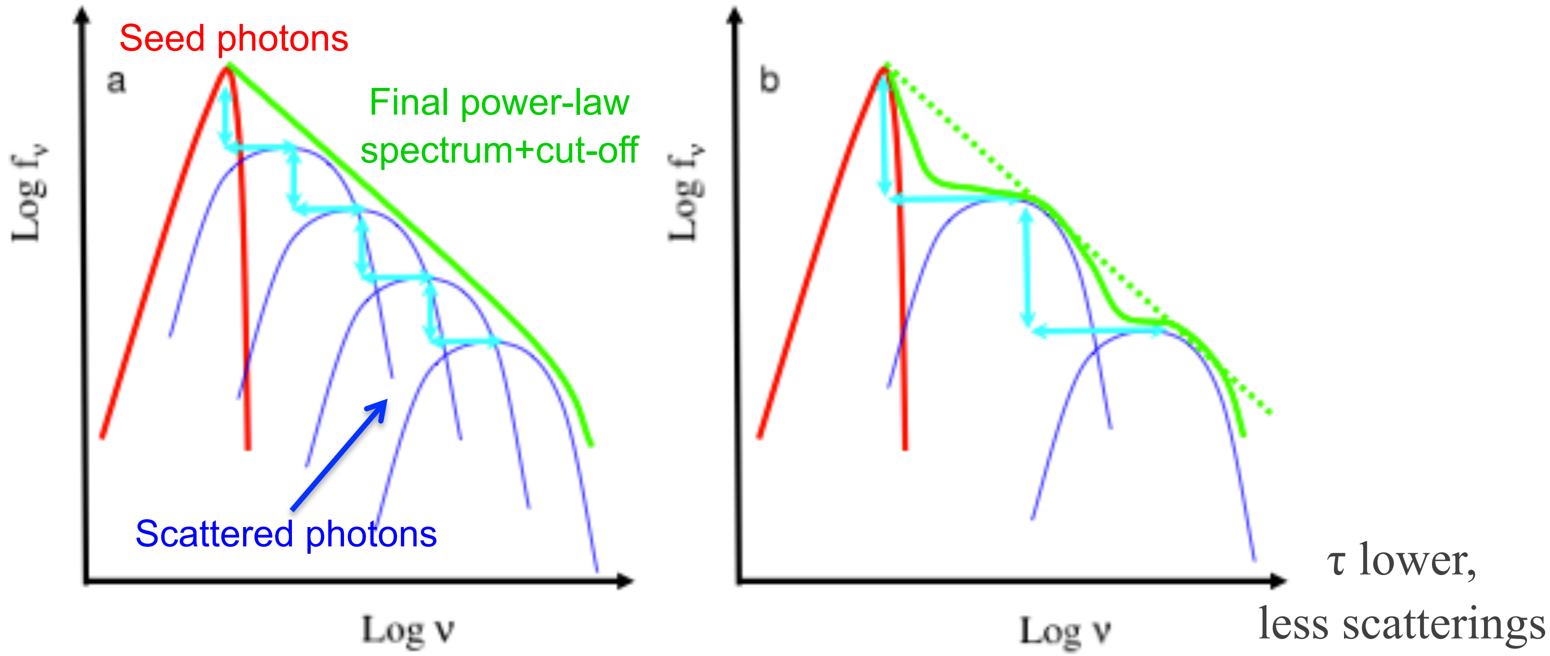

Seed photons are up-scattered, then become the "new" seed photons for following scatterings ➔ the overall spectrum resembles that of a powerlaw

Thermal Comptonization: electrons have a Maxwellian distribution. Cut-off in the powerlaw when the process of transferring energy from electrons to photons is not efficient anymore ($E_{cut\text{-}off} \approx kT_{electrons}$)

High-energy emission from AGN: thermal Comptonization (IV)
Type 1 vs. Type 2 AGN

Seyfert X-Ray Spectra

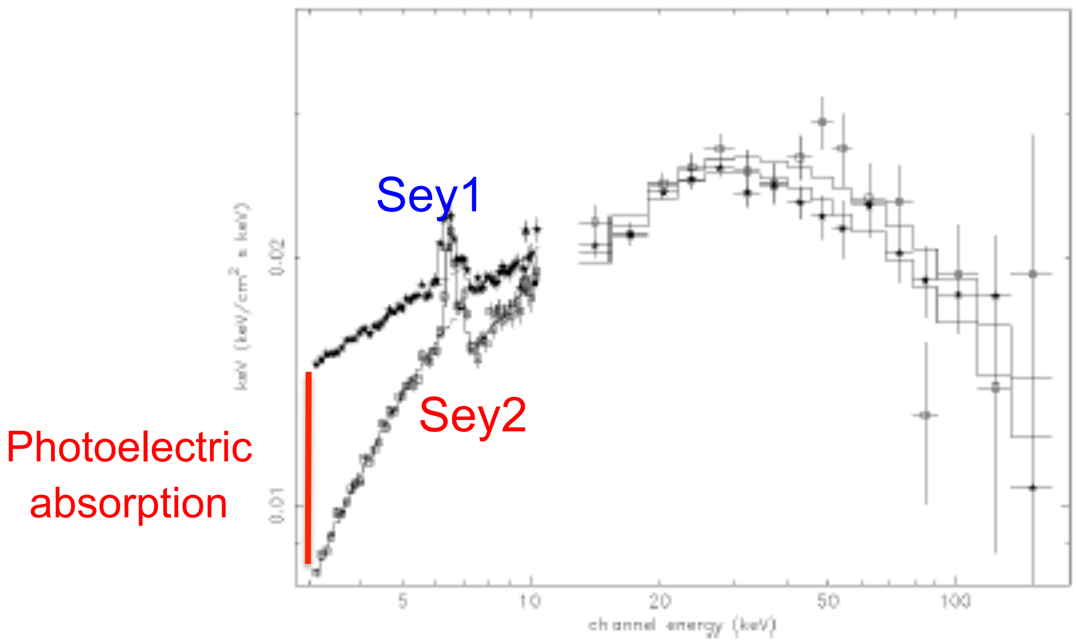

(Average Sy 1 and Sy 2 spectra from *BeppoSAX* Malizia et al., 2003, Fig. 4)

Spectra of Sy 1 and Sy 2 are very similar, except for lower $N_{\rm H}$ in Sy 2

High-energy emission from AGN: Reflection

[II] Compton reflection hump: **Reflection**: power-law photons produced by Inverse Compton are partly scattered by the disc and partly arrive to the observer.

Approx. half of the photons from Comptonization reach the observer, half are directed to the accretion disc ➔ reflection + fluorescence emission

Bump due to photoelectric absorption at low energies, and Compton recoil at high energies (i.e., photons penetrate deeply in the disc because of the Klein-Nishina cross section and lose energy, hence absorption becomes relevant again)

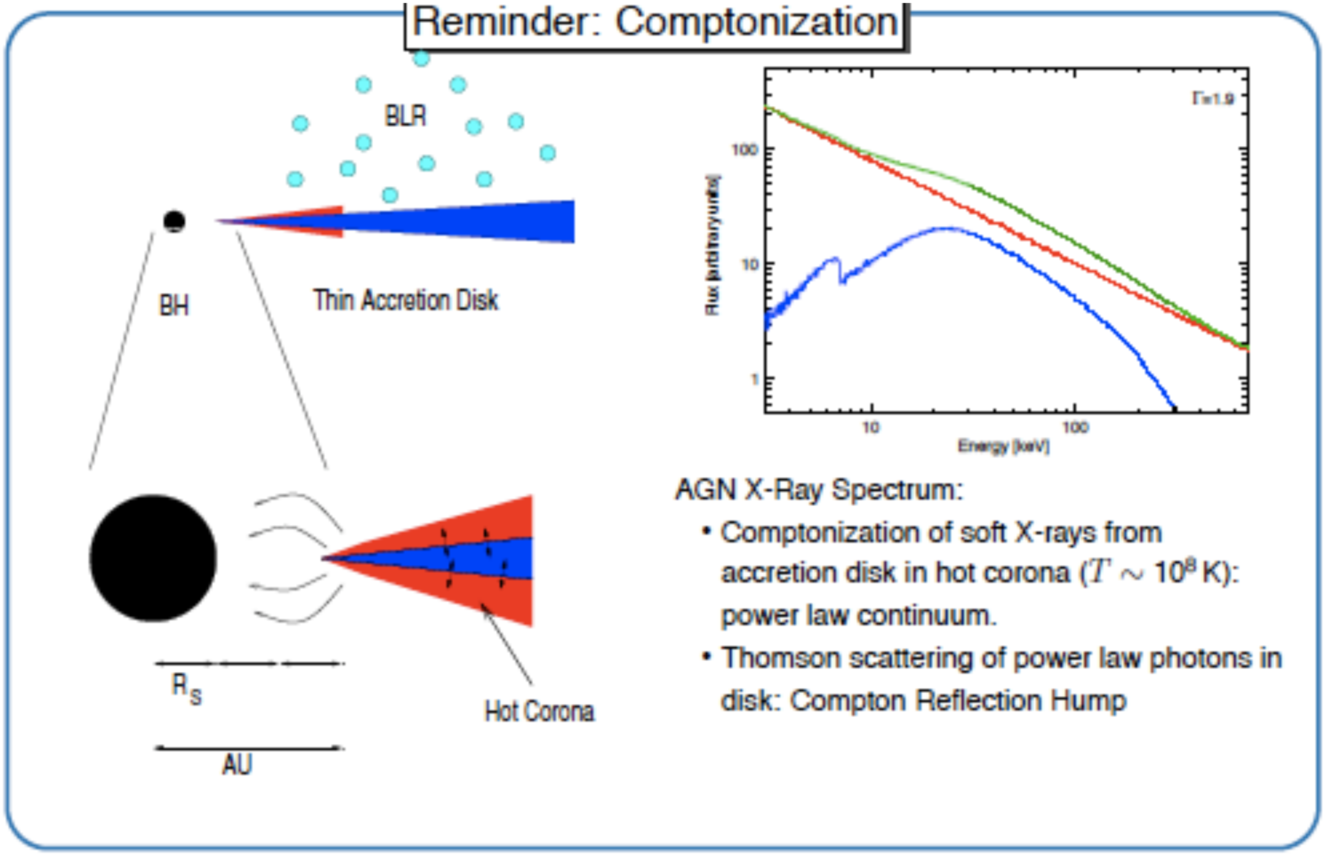

High-energy emission from AGN: Fluorescence emission

[III] Fluorescence Fe Kα emission (neutral or ionized, depending on the ionization status of the matter)

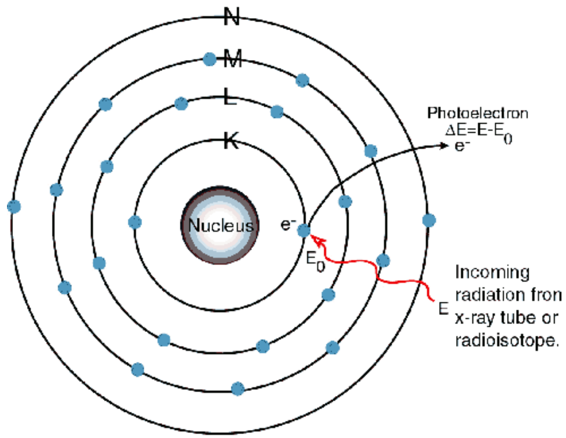

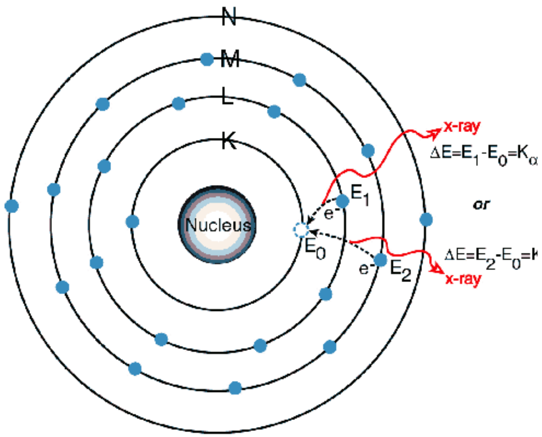

Reminder: Comptonization

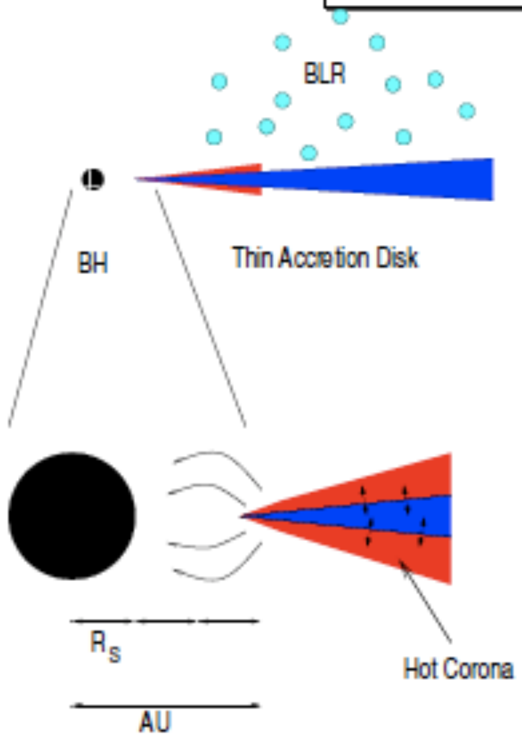

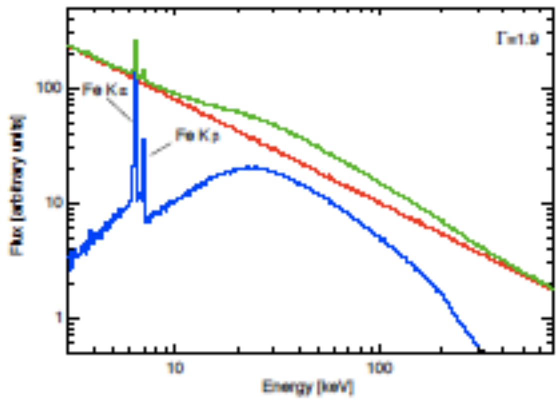

AGN X-Ray Spectrum:

- Comptonization of soft X-rays from accretion disk in hot corona ($T \sim 10^8$ K): power law continuum.
- Thomson scattering of power law photons in disk: Compton Reflection Hump
- Photoabsorption of power law photons in disk: fluorescent Fe $K\alpha$ Line at $\sim$6.4 keV

Fluorescence line

Photoelectric Absorption

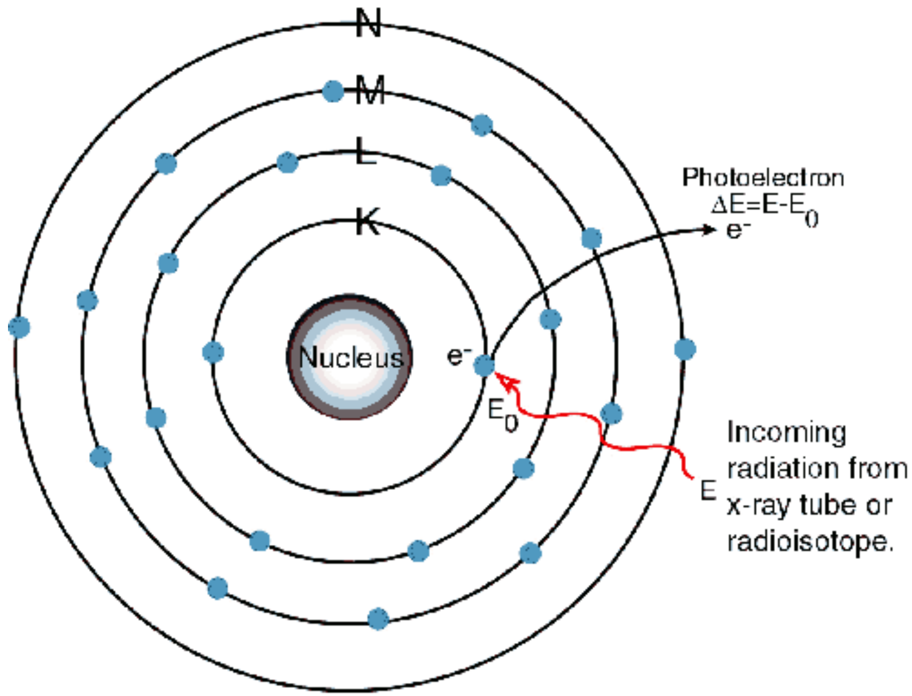

Fluorescence (+ Auger effect)

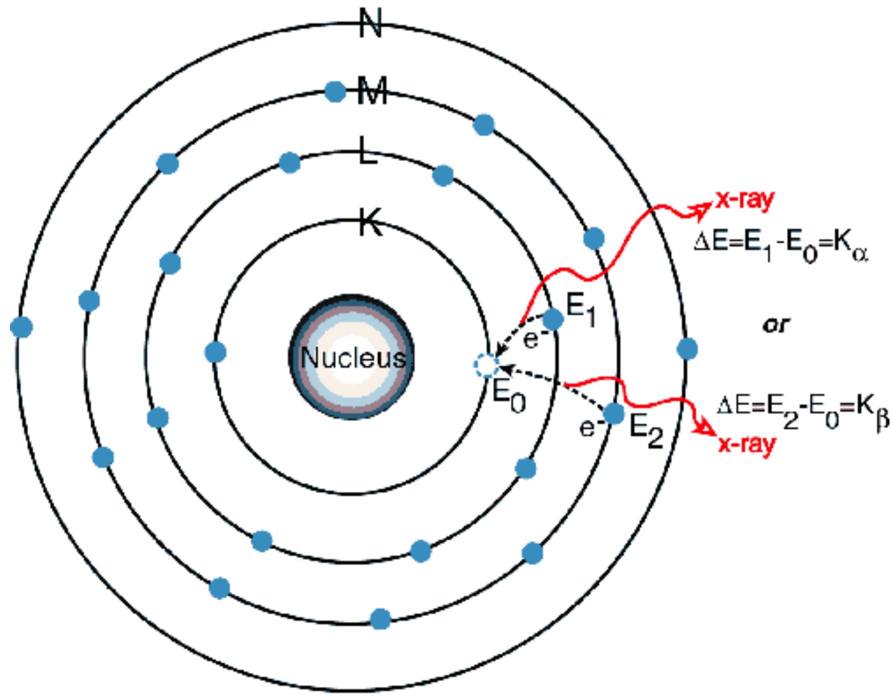

High-energy emission from AGN: summary of the components

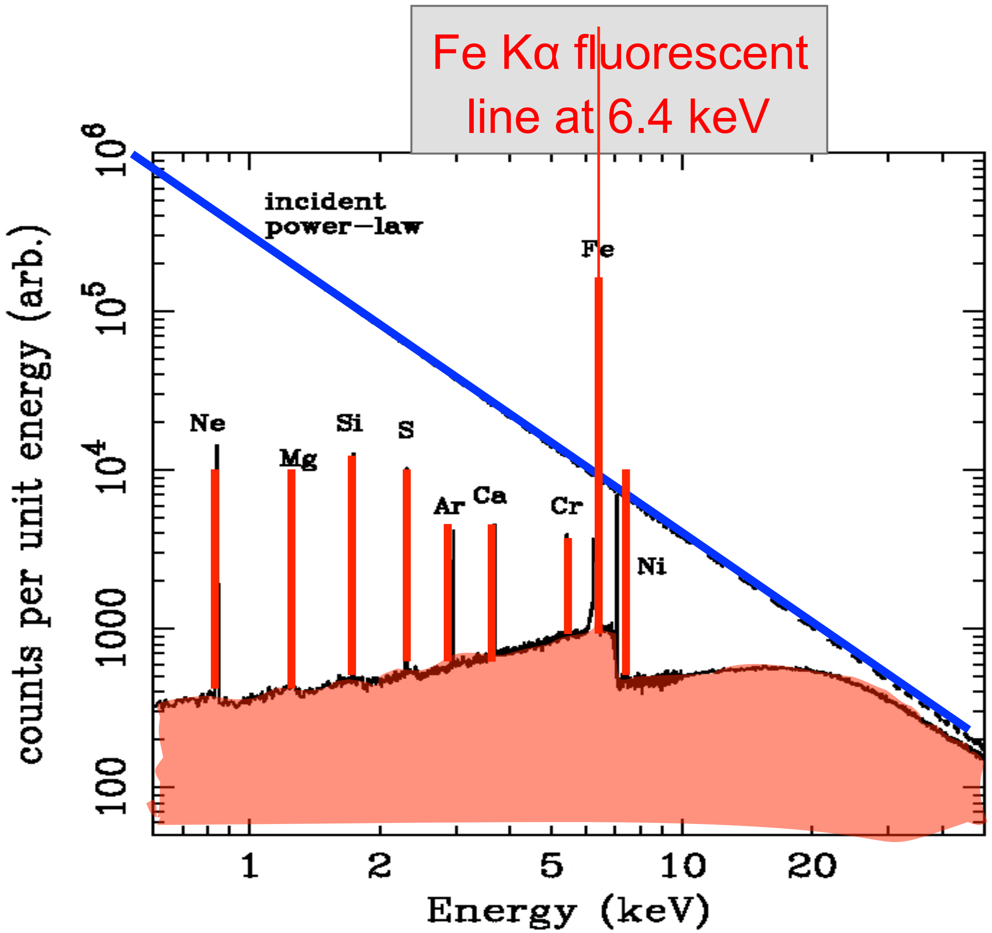

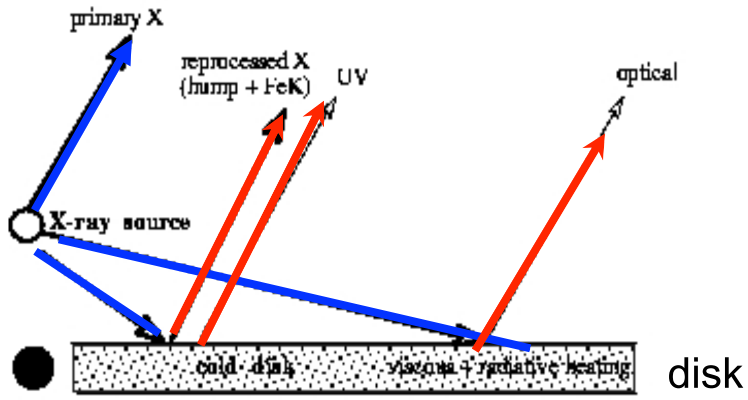

Lamp-post model

High-energy emission from AGN

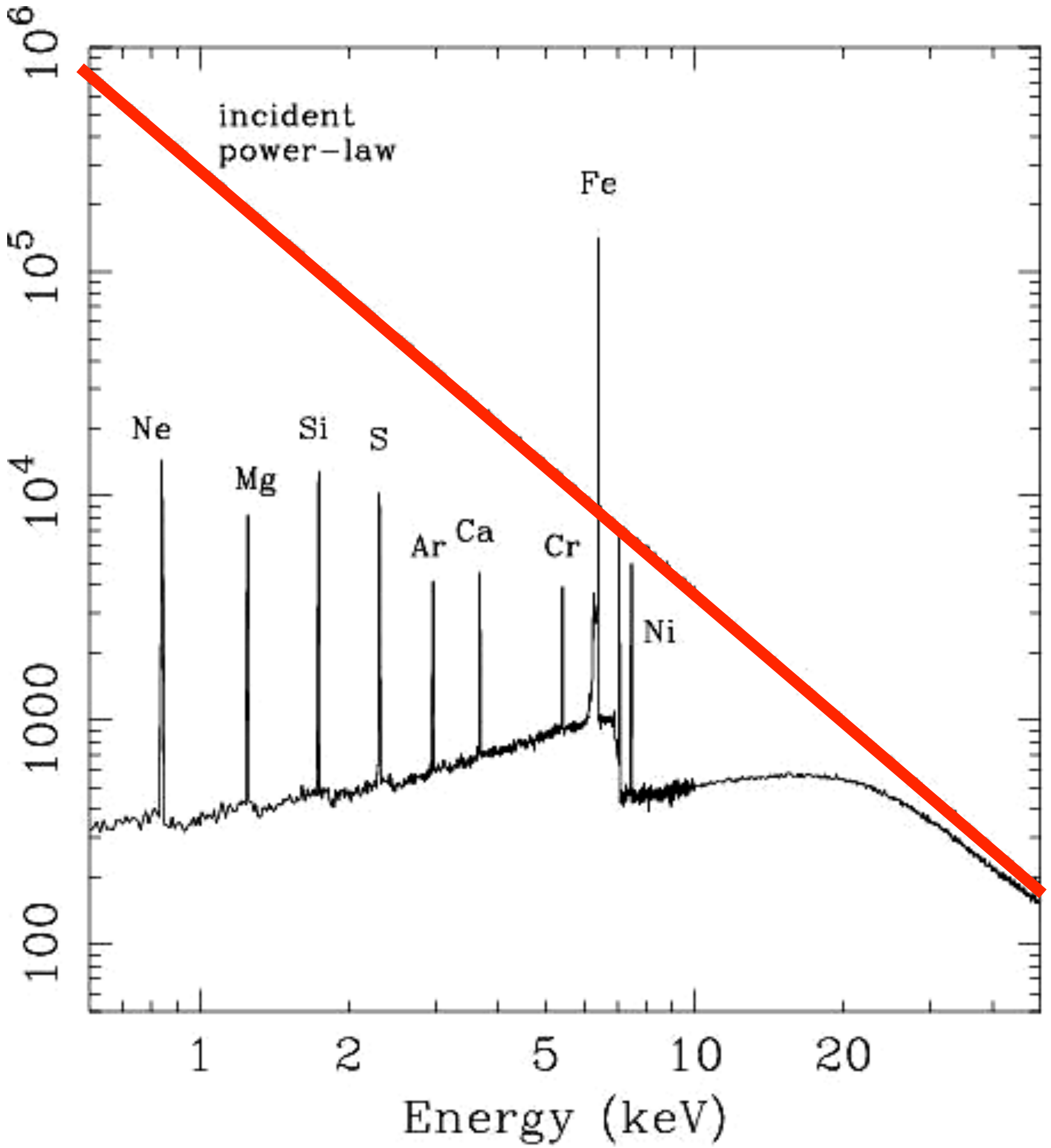

The resulting X-ray reflection spectrum comprises:

- a plethora of fluorescence emission lines from the most abundant metals
- a Compton hump at 20-30 keV due to Compton scattering

In general, the disc upper layers (where reflection arises) are irradiated from above but also heated from below by the main body of the AD ➔ complex structure ➔ radiative transfer problem

One possibility is to mantain the constant density assumption assuming thermal and ionization equilibrium and solve the radiative transfer equations

Ionization parameter

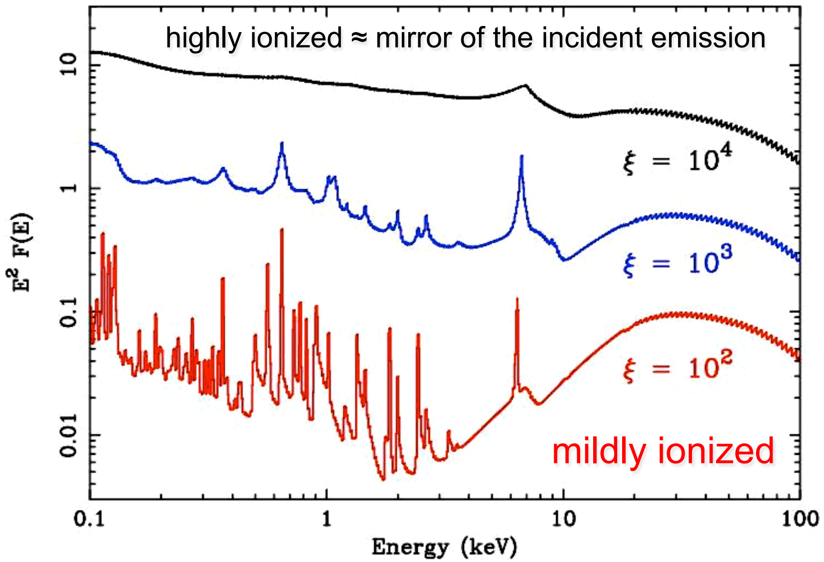

Reflection spectrum in case of ionized matter

$$\xi(r) = \frac{4\pi F_X}{n(r)} = \frac{L_X}{nR^2} = \frac{L_X}{N_H R} \;\; [\mathrm{erg\ cm/s}]$$

In astrophysical cases, the ionization parameter has a non-uniform radial profile

High-energy emission from AGN

Seyfert X-Ray Spectra

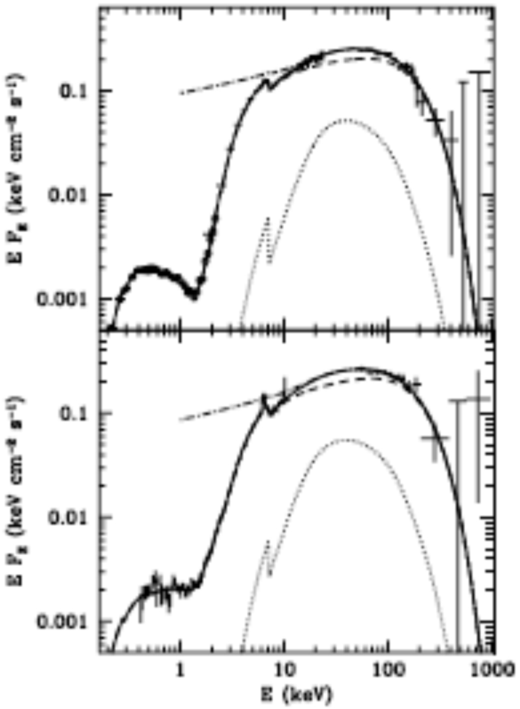

Comptonization explains broad-band Seyfert spectra very well

Example: Fits of Comptonization models to broad-band spectrum of Seyfert 1 galaxy NGC 4151 showing all three components:

- $kT_e \sim 88^{+55}_{-26}$ keV
- $N_H \sim 7 \times 10^{22}\,\mathrm{cm}^{-2}$ and $13 \times 10^{22}\,\mathrm{cm}^{-2}$, respectively
- Reflection factor: $\Omega/2\pi = 0.43$ (assumed; consistent with Fe line, but not significantly detected in these data [but in other AGN]).

Note strong absorption present in Seyfert 1 X-ray spectra!

(Zdziarski, Johnson & Magdziarz, 1996)

Comptonization seems to work up to high energies (as already experienced in mid ’90)

Need for broad-band X-ray spectra to reveal and characterize all of the components
(better if all data come from the same satellite)

Broad (relativistic) iron lines

Relativistic iron line profile (I)

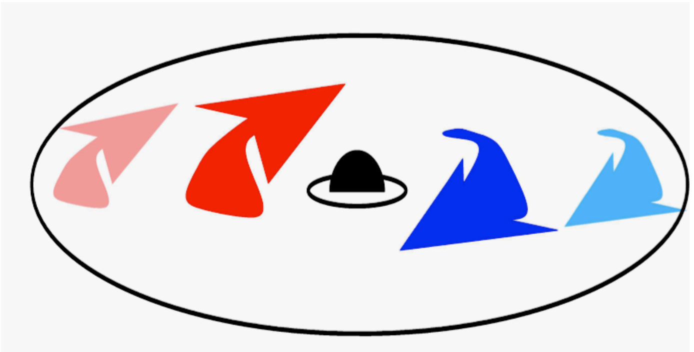

Consider a ring on the disc emitting a narrow Fe line

Doppler effect produces a symmetric double-peaked profile

relativistic beaming enhances the blue peak

transverse Doppler and GR redshift shift the overall line profile to the red

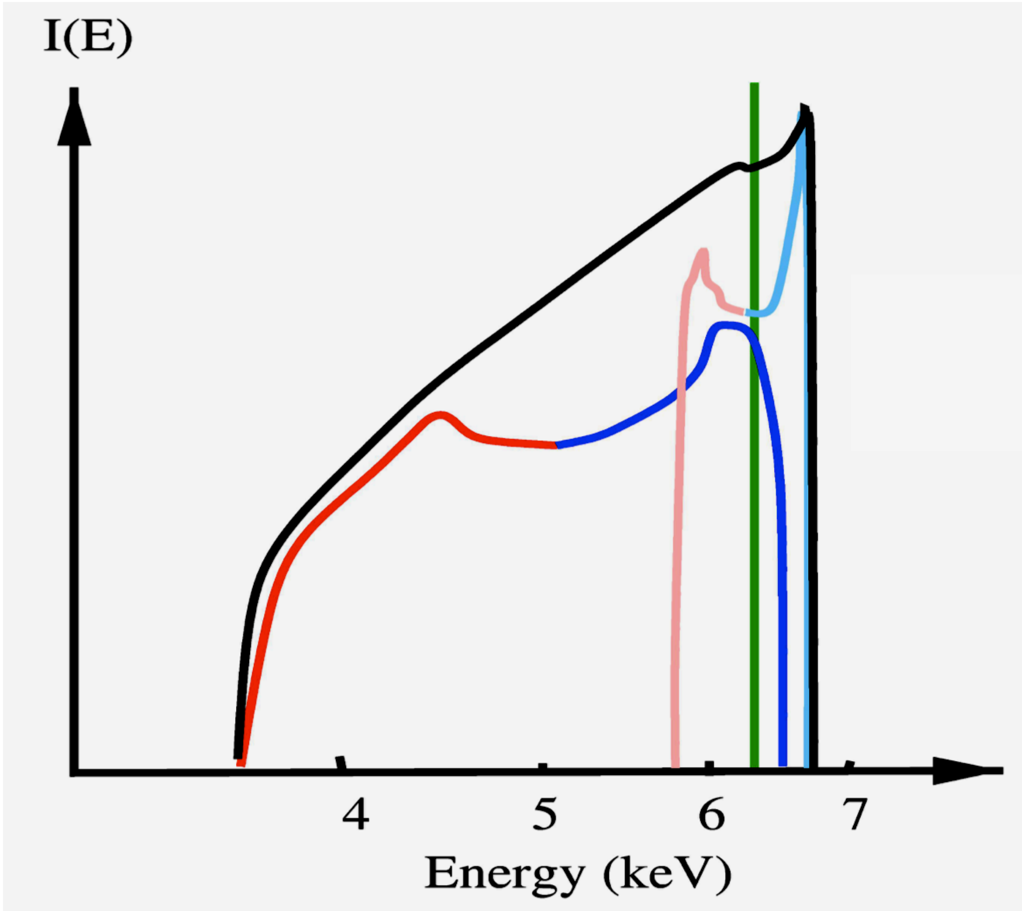

Relativistic iron line profile (II)

Newtonian

Special relativity — Transverse Doppler shift; Beaming

General relativity — Gravitational redshift

Line profile

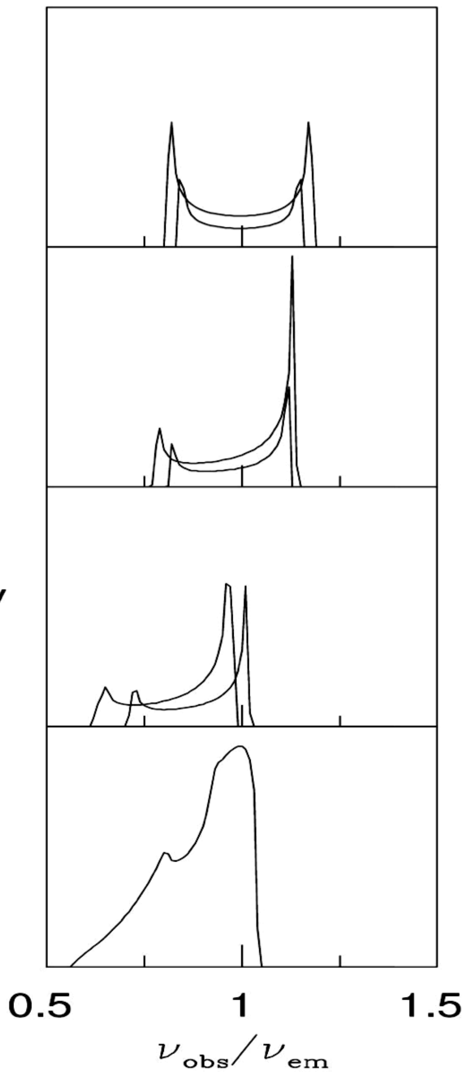

The relativistic line profile depends on:

- inner disc radius
- inclination of the disc
- emissivity profile

Relativistic iron line profile (III) − Inner disc radius

The inner disc radius is generally assumed to be the **ISCO**

Schwarzschild BH: $R_{in}=6R_g$

Kerr BH: $R_{in}=1.24R_g$

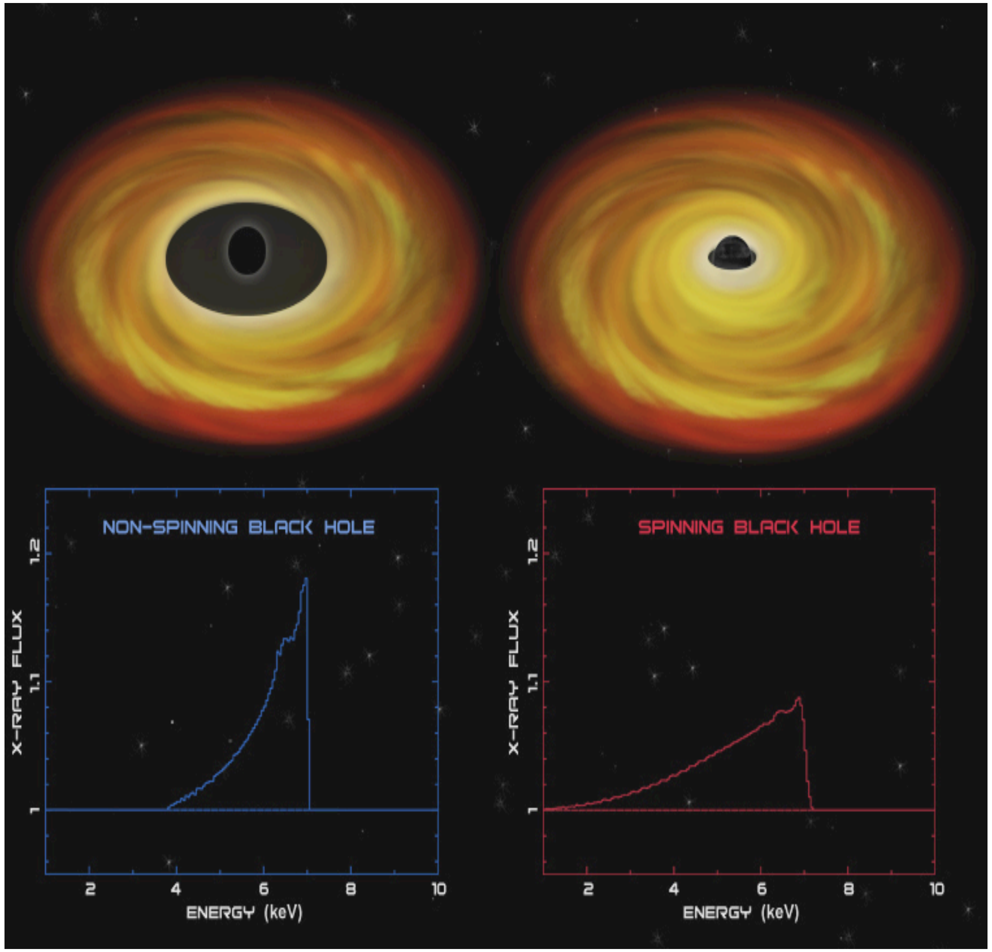

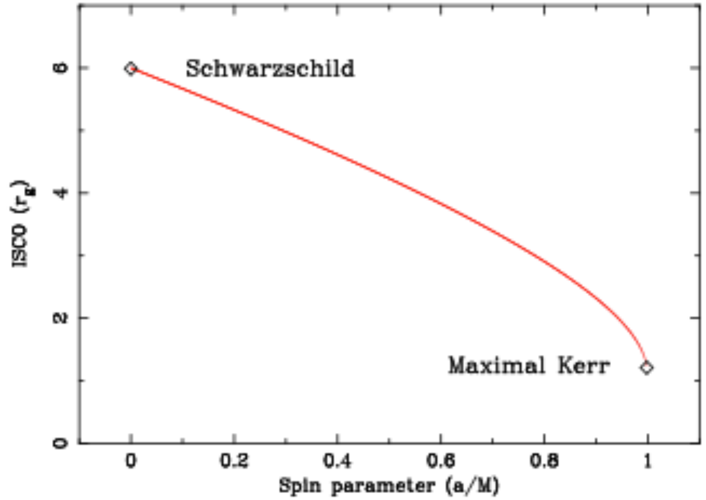

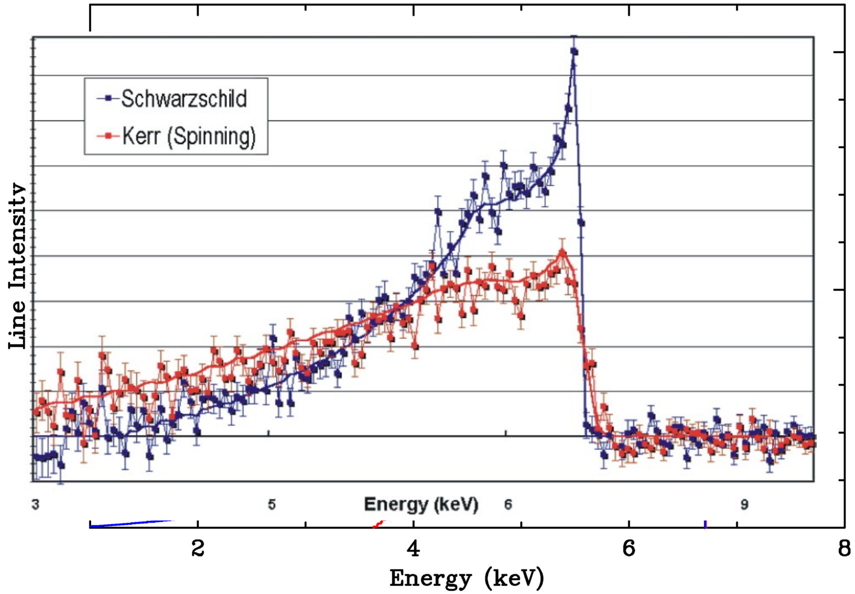

Relativistic iron line profile (IV)
Inner disc radius from X-ray real data

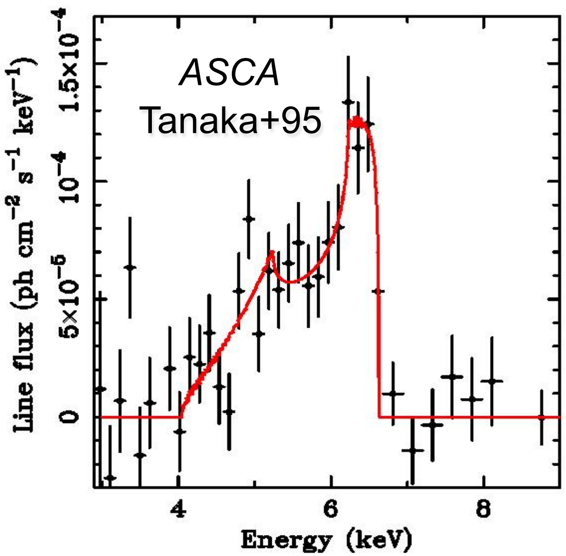

First evidence: MCG-6-30-15 from *ASCA* data (Tanaka+95) − 5 day-obs.

i≈30 deg
Steep emissivity profile
R_{in}≈2R_g, significant BH spin

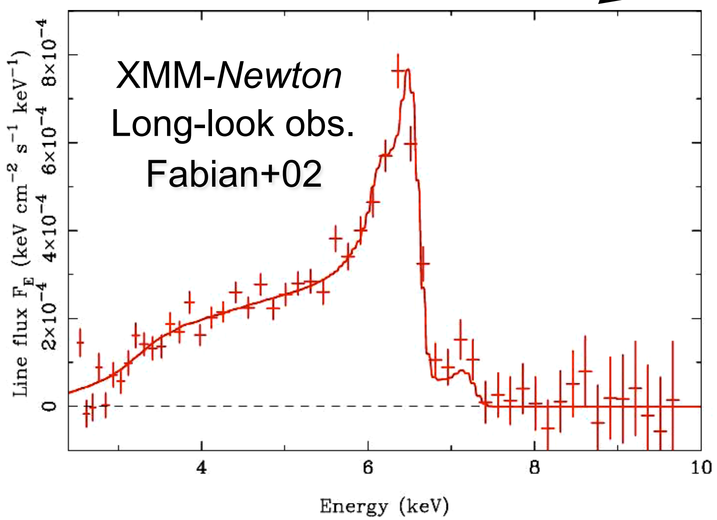

Large (a>0.985) BH spin

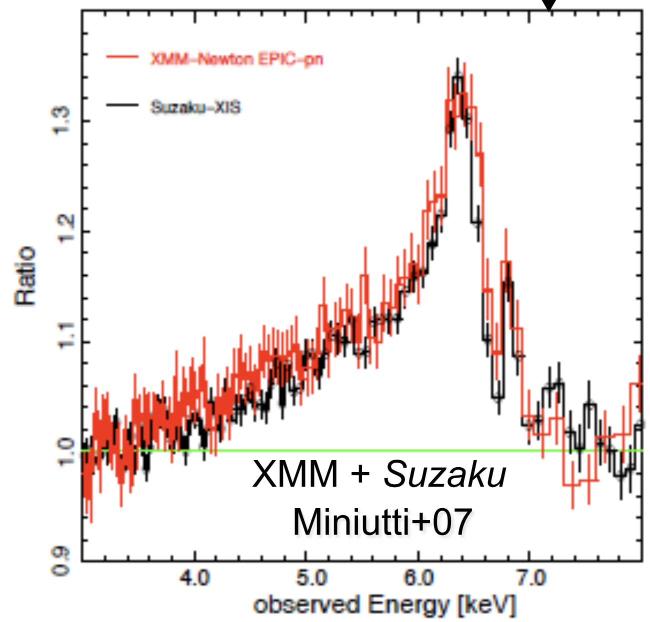

Relativistic iron line profile (V)
Inner disc radius from X-ray real data

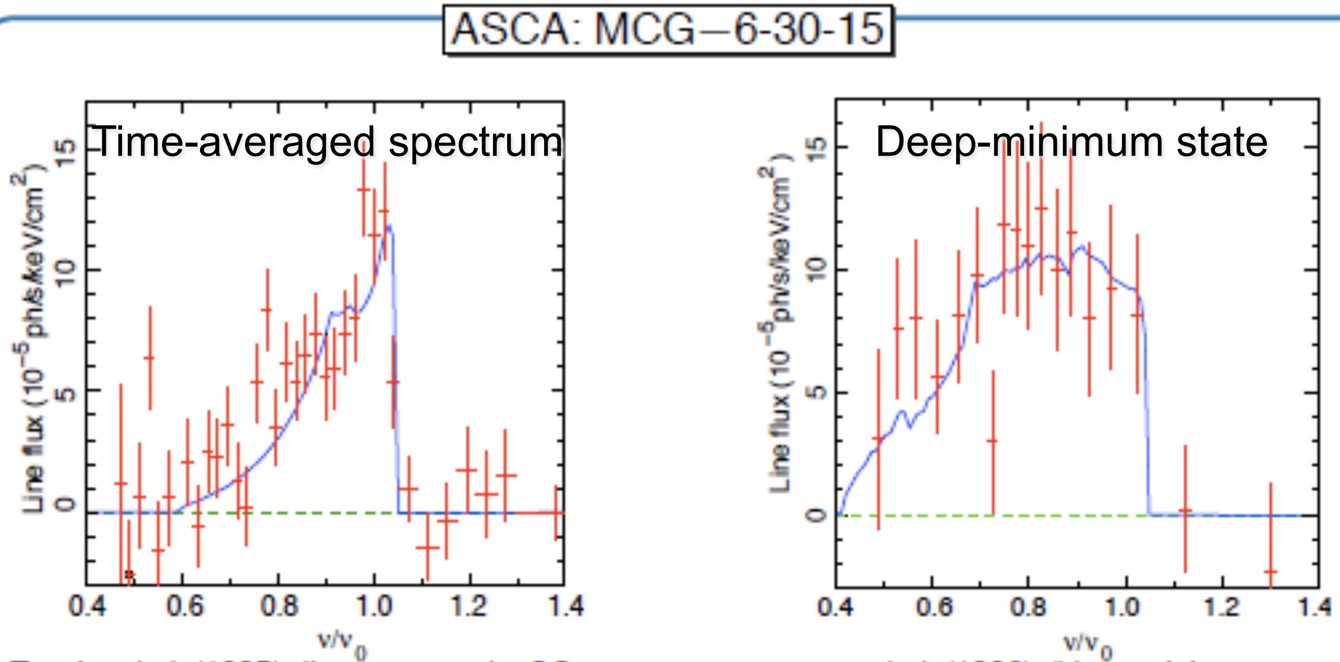

Tanaka et al. (1995): time averaged *ASCA* spectrum: line skew symmetric
⟹ Schwarzschild black hole.

Iwasawa et al. (1996): "deep minimum state": extremely broad line
⟹ Kerr Black Hole.

Later confirmed with *BeppoSAX* (Guainazzi et al., 1999) and *RXTE* (Lee et al., 1999).

Relativistic iron line profile (VI) − Inclination angle of the disc

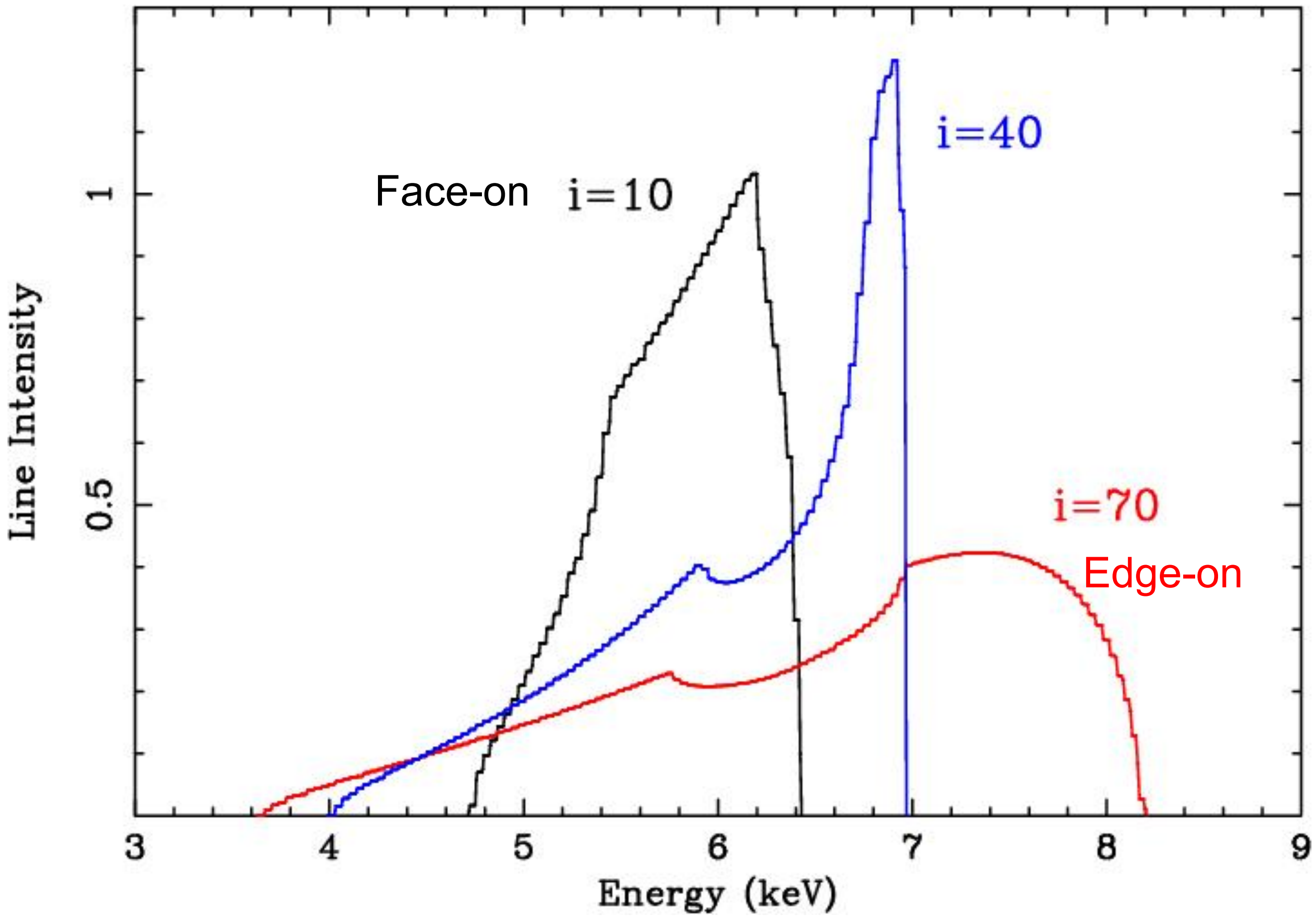

Relativistic iron line profile (VII) − Emissivity profile

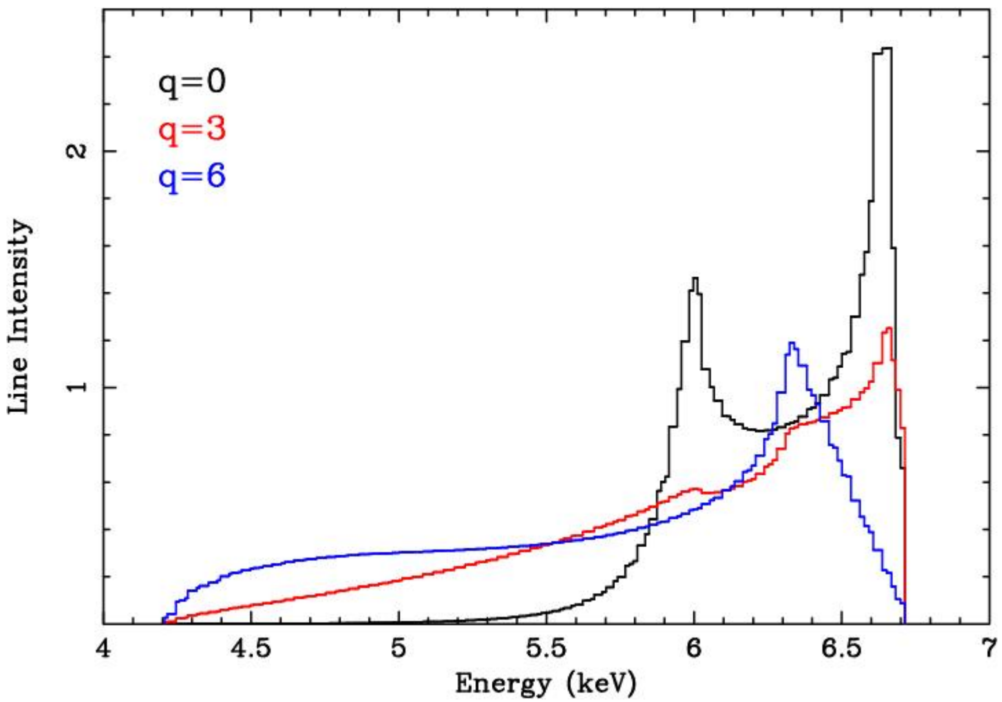

Emissivity profile:

$$\varepsilon(r) \propto r^{-q}$$

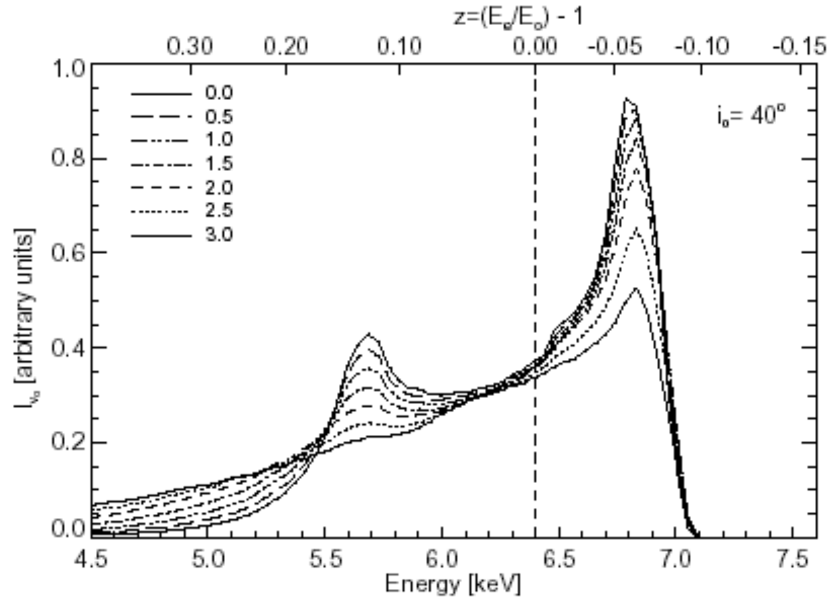

Relativistic iron line profile (VIII) – Black Hole spin

Reminder: Relativistic Lines

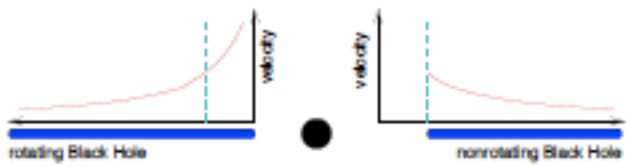

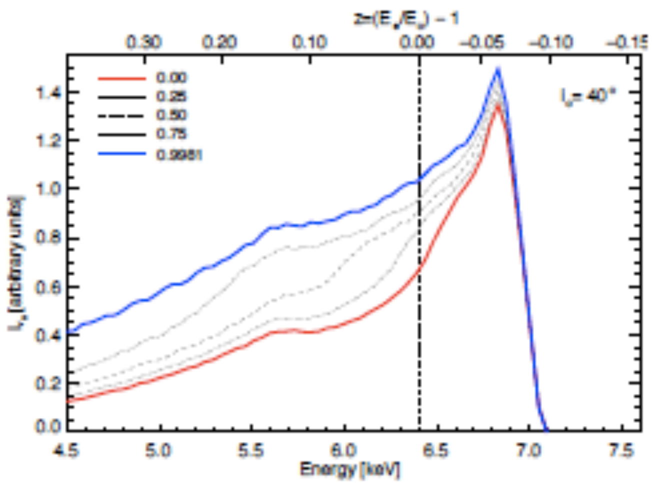

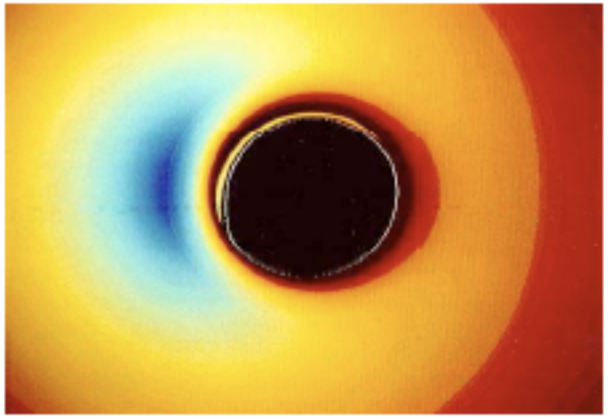

Total observed line profile affected by

- grav. Redshift
- Light bending
- rel. Doppler shift
- emissivity profile
- spin of black hole

Detailed physical models required to fit these lines and good data, besides a good knowledge of the underlying spectral continuum → spectral component degeneracy may be an issue

Relativistic iron line profile (IX) – ISCO

	a	r_{isco}/r_g	η
	-1.0	9.0	0.038
Non-rotating (Schwarzschild) BH	0	6.0	0.057
	0.1	5.67	0.061
	0.5	4.23	0.082
	0.9	2.32	0.156
Rapidly-rotating (Kerr) BH	0.998	1.24	0.321
	1.0	1.00	0.423

high η means less mass available for M_{BH} growth

η=radiative efficiency
J=angular momentum=IΩ, where Ω=angular velocity
J/M=specific angular momentum
j=a/M=dimensionless angular momentum per unit mass
a=dimensionless angular momentum (sign=direction of rotation)

"SPIN" of the BH

$$j = Jc / GM^2_{BH} = a / M_{BH} \rightarrow a = Jc / GM_{BH} = J / M_{BH} r_g c$$

Warm absorber

Warm absorber (I)

Warm Absorbers

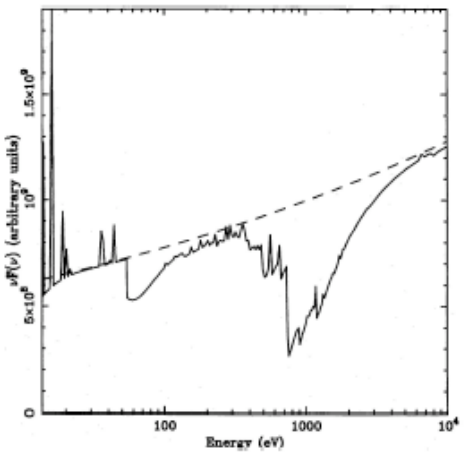

(Reynolds & Fabian, 1995, Fig. 1)

Photoionization calculations: Warm absorbers show strong O VII and O VIII edges at 739 eV and 839 eV.

First resolvable in 1990s with *ASCA*:

Nandra & Pounds (1994): Warm absorbers are found in ∼50% of all Seyfert 1s.

In ≈50% of Sey 1s

Prominent ionized O edges (E≈0.74−0.84 keV) in low-resolution X-ray spectra

More detailed studies and more line profiles from recent X-ray grating spectroscopy

MR 2251-178

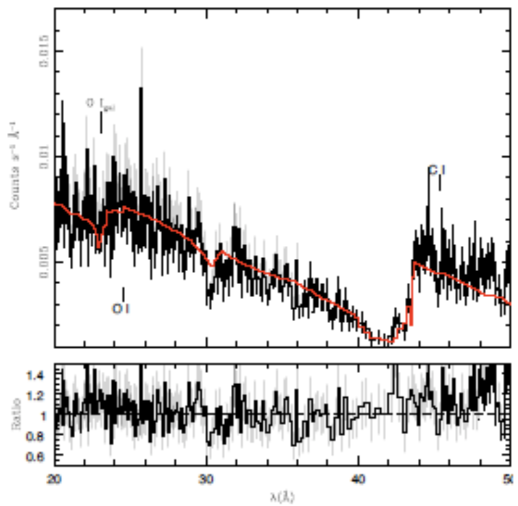

(MR 2251−178; Ramirez et al., 2008, O edge region)

With high-resolution gratings spectroscopy on *XMM* and *Chandra*, warm absorber can be studied in much greater detail than before.

Warm absorber (II)

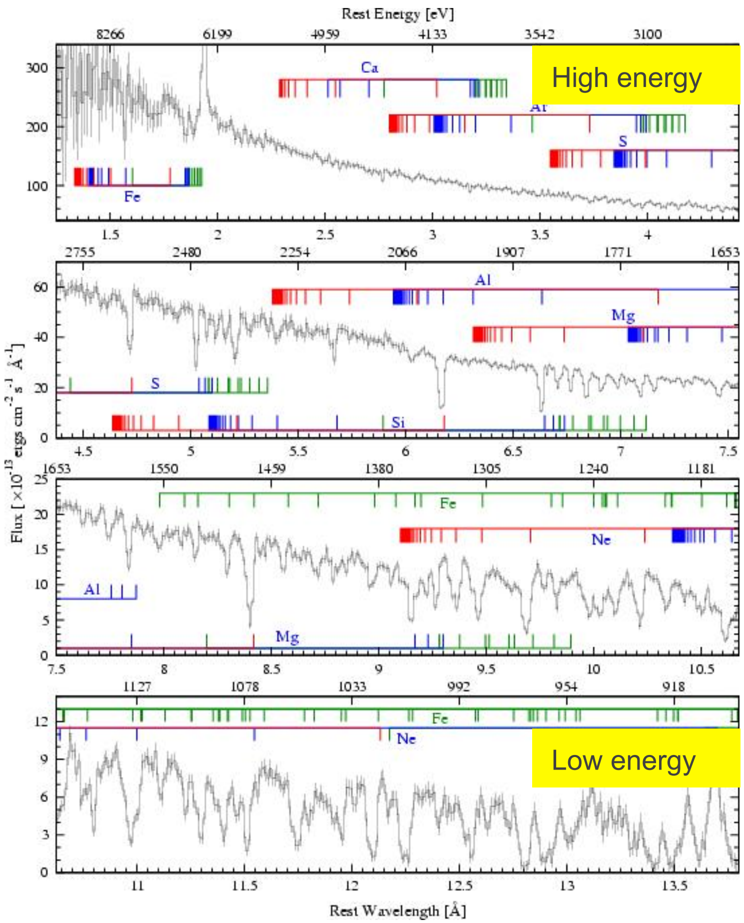

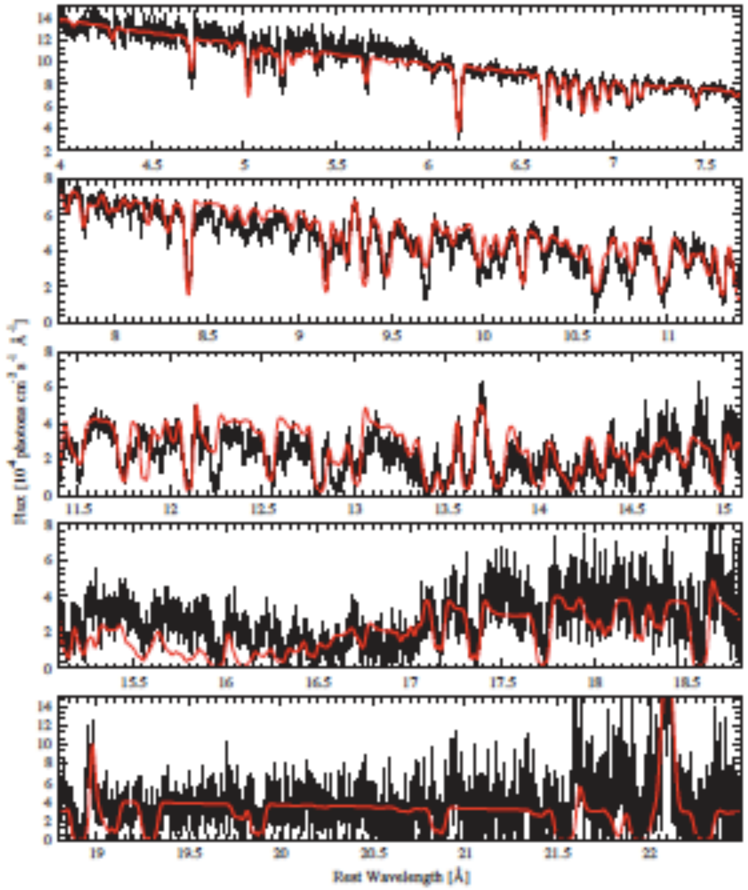

NGC 3783 (≈900 ks *Chandra*) − Kaspi et al. (2002) + Netzer et al. (2002)

➔ Multiple ionization and kinetic components with outflows of ≈100-1000 km/s

Warm absorber (III)

The highly ionized lines in warm absorber spectra are blue-shifted
➔ wind from the accretion disc?

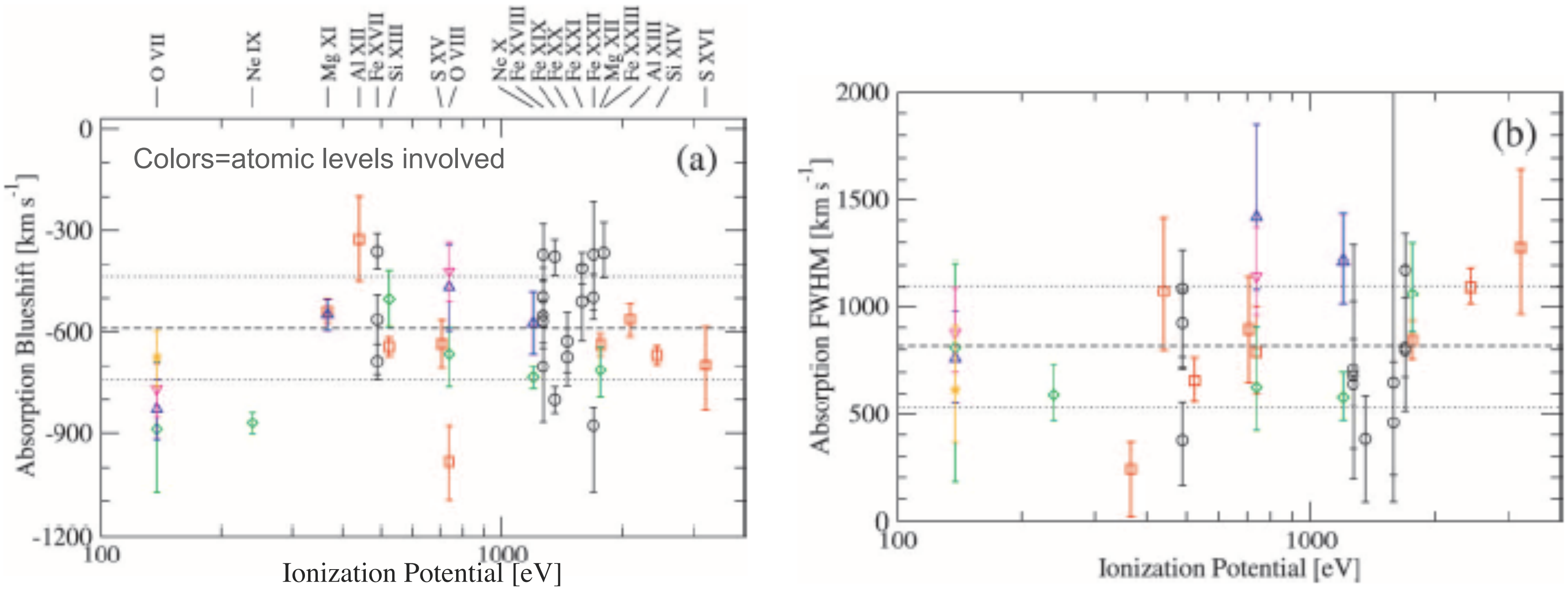

NGC 3783 (≈900 ks *Chandra*) − Kaspi et al. (2002)

From warm absorbers to ultra-fast outflows (I)

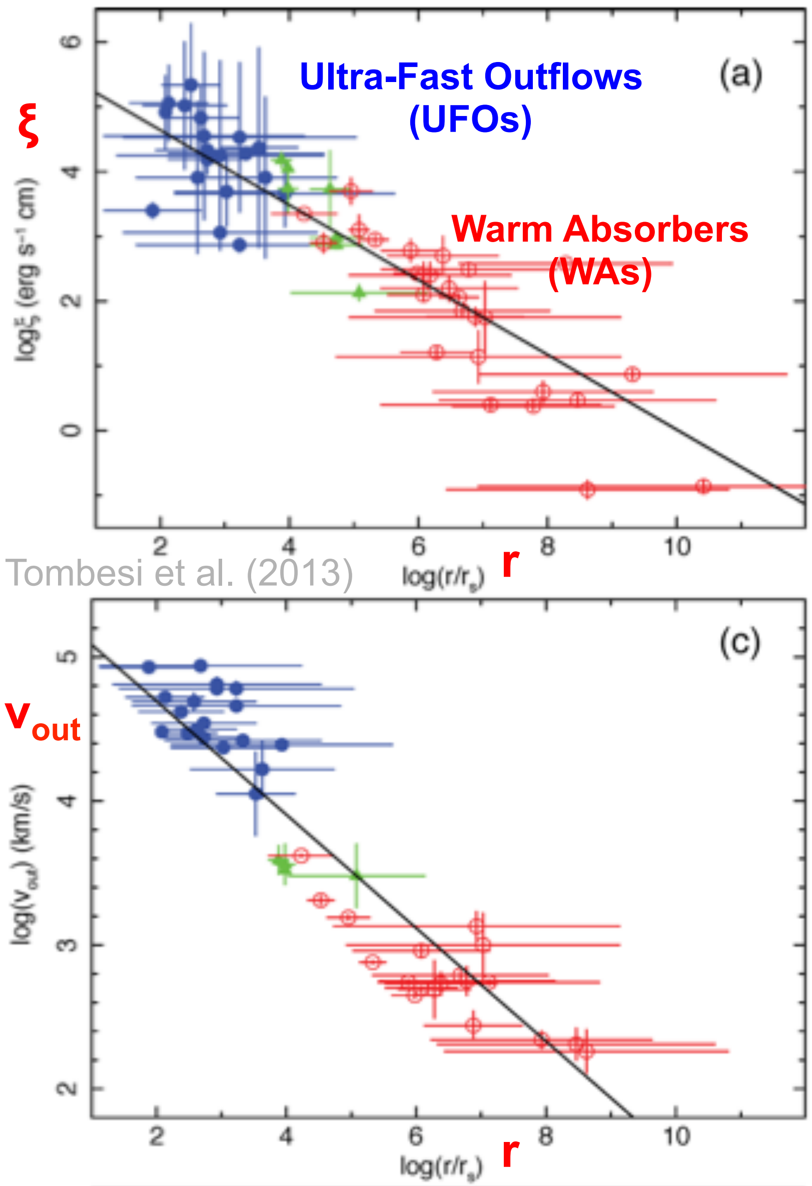

Tombesi et al. (2013)

Warm absorbers (WAs; v≈1000 km/s) (e.g., Blustin+05)

Ultra-fast outflows (UFOs; v≈0.05c up to 0.6c) (e.g., Tombesi+, Gofford+, Chartas+, Lanzuisi+12, […])

The closer the absorber to the BH, the higher ionization (ξ), column density (N_H) and outflow velocity (v_{out})

WAs and UFOs at the two ends of the parameter space

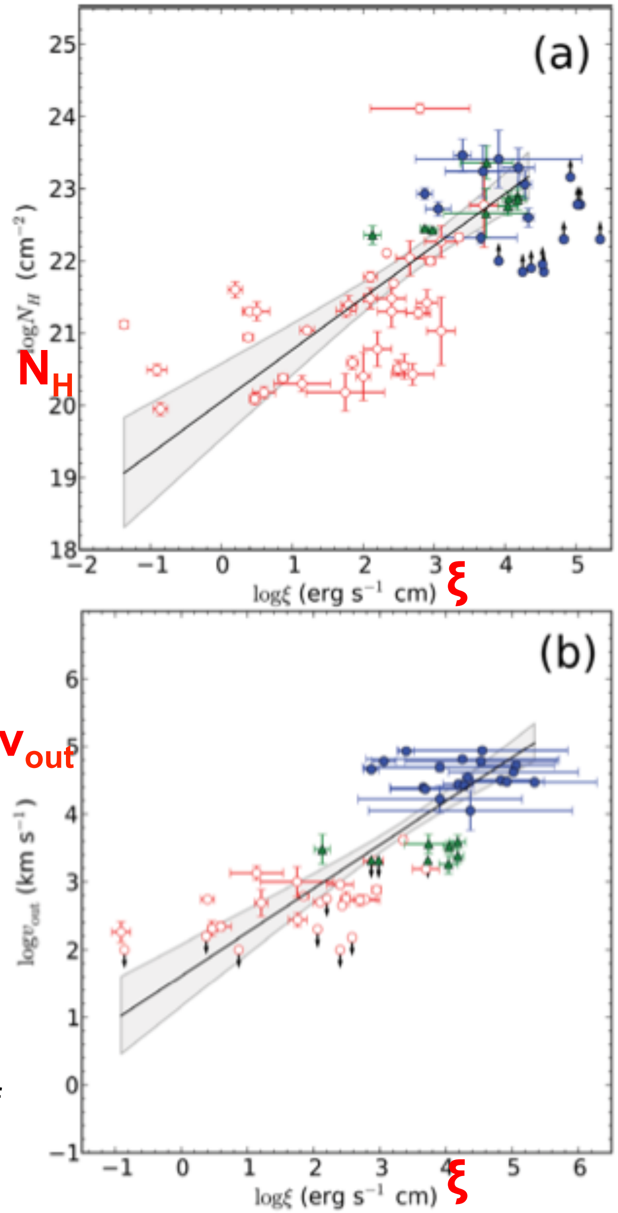

From warm absorbers to ultra-fast outflows (II)

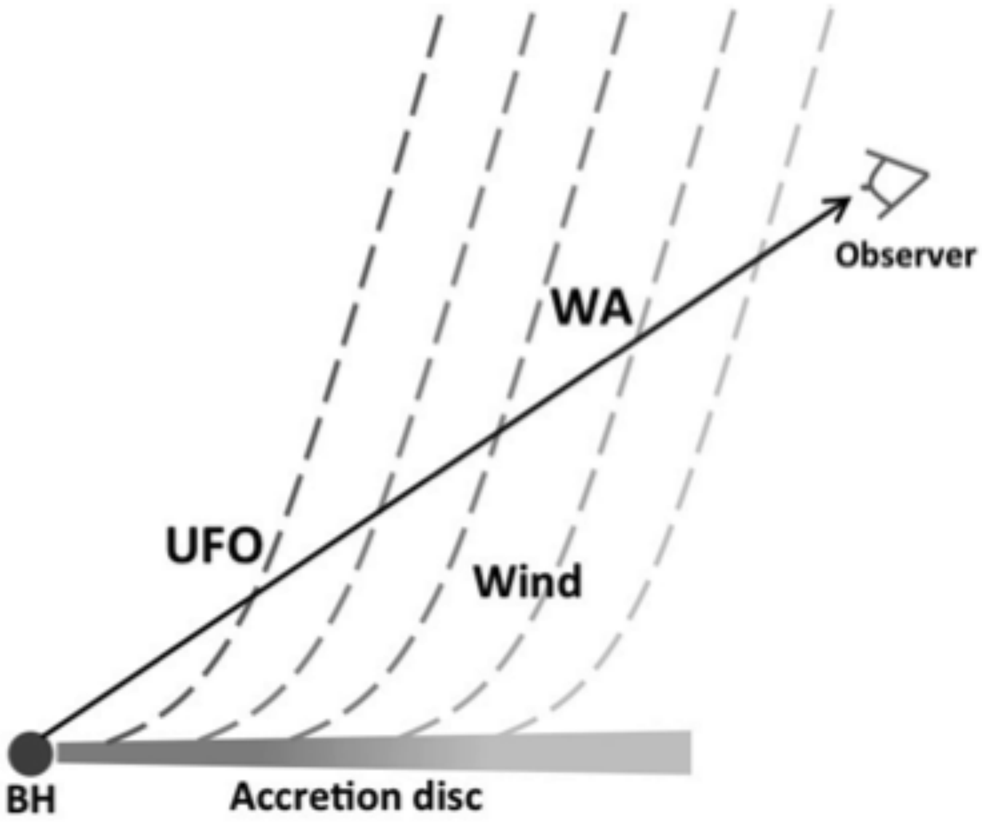

Tombesi et al. (2013) − see also Kazanas et al. (2012)

A single, stratified large-scale outflow?

Radiation pressure and magneto-hydrodynamical processes responsible for the acceleration

Launch location: UFOs from the inner accretion disc (see also BALQSOs)

High mechanical power implied (≈0.5% of L_{bol} for UFOs) ➔ feedback issues

The torus can be an extension of the outer accretion disc

Ultra-fast outflows (I)

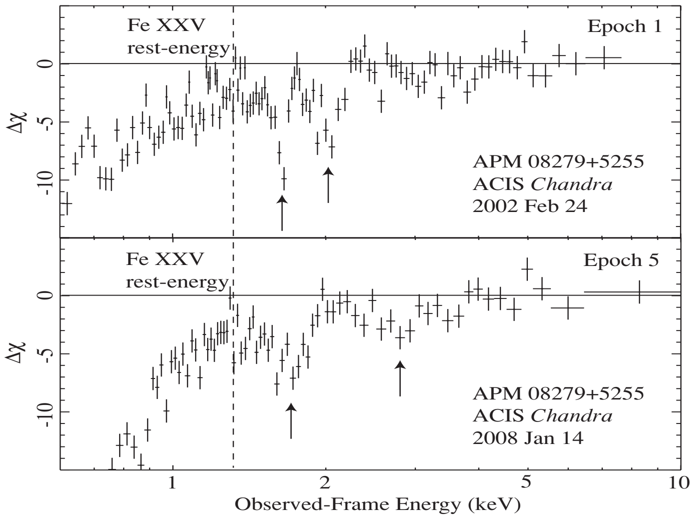

Chartas+09; Saez+09

APM 08279+5255 (z=3.91)

$V_{out} \approx (0.2\text{-}0.76)c$

Needs for high statistics for a proper modeling.

Mostly Seyferts at low z or lensed QSOs at high z

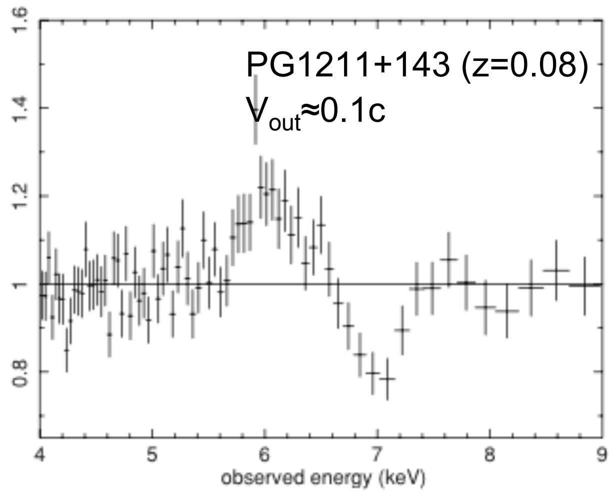

PG1211+143 (z=0.08)

$V_{out} \approx 0.1c$

Pounds & Reeves09

Nardini+15

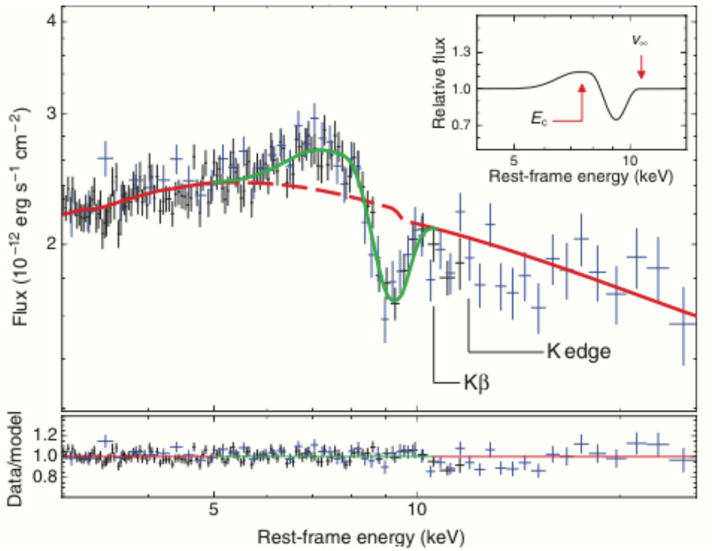

PDS456 (z=0.18)

$V_{out} \approx 0.3c$

Lanzuisi+12

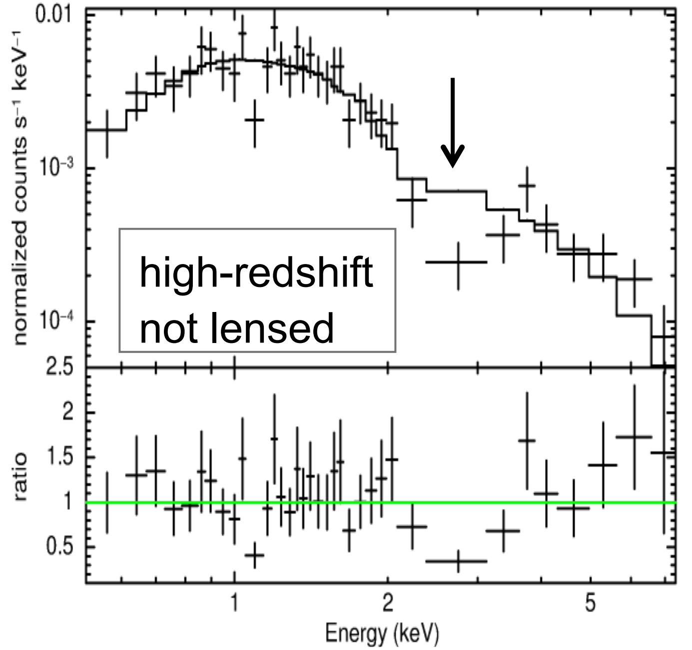

HS1700+6416 (z=2.73)

$V_{out} \approx (0.1-0.6)c$

Ultra-fast outflows (II)

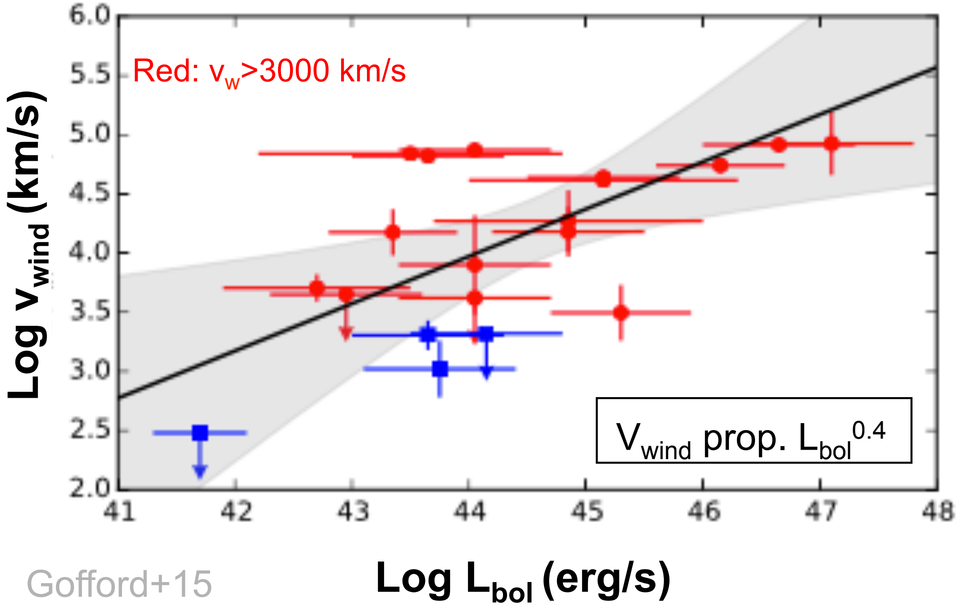

Gofford+15

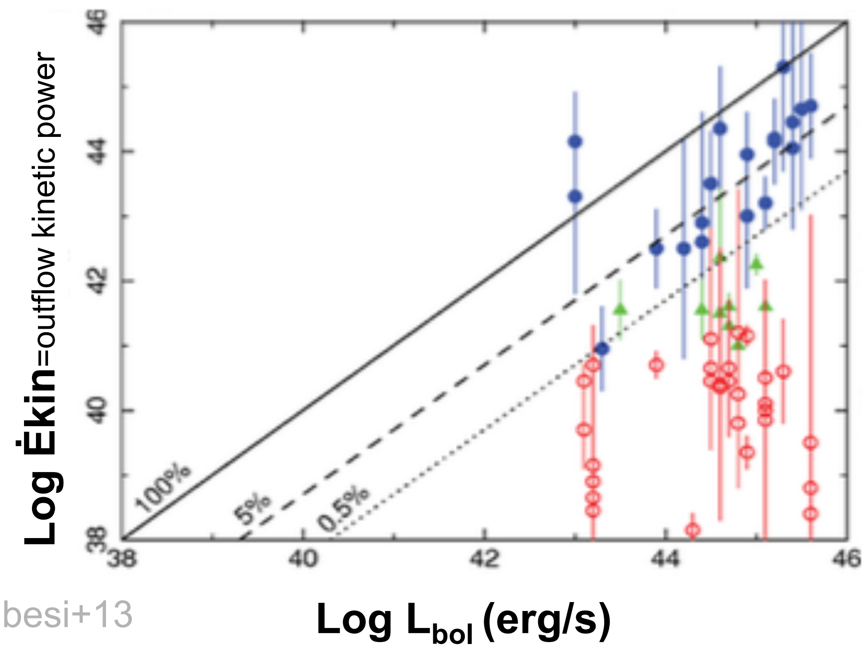

Tombesi+13

Ultra-fast outflows (UFOs)

- Detected in **≈50%** of nearby radio-quiet AGN with good spectral quality
- Similar fraction in RL AGN, still winds are the main actors
- Independent XMM-*Newton* vs. *Suzaku* detection (Tombesi+, Gofford+)
- $<v_{wind}>\approx 0.1c$
- Highly ionized ($<\log\xi>\approx 4$) and large column densities ($<\log N_{H}>\approx 23$)
- Variable in EW and velocity (Tombesi+)
- Mechanical power ≈5−10% L_{bol}, hence potentially important for **feedback**

Linking X-ray outflows with molecular outflows. I

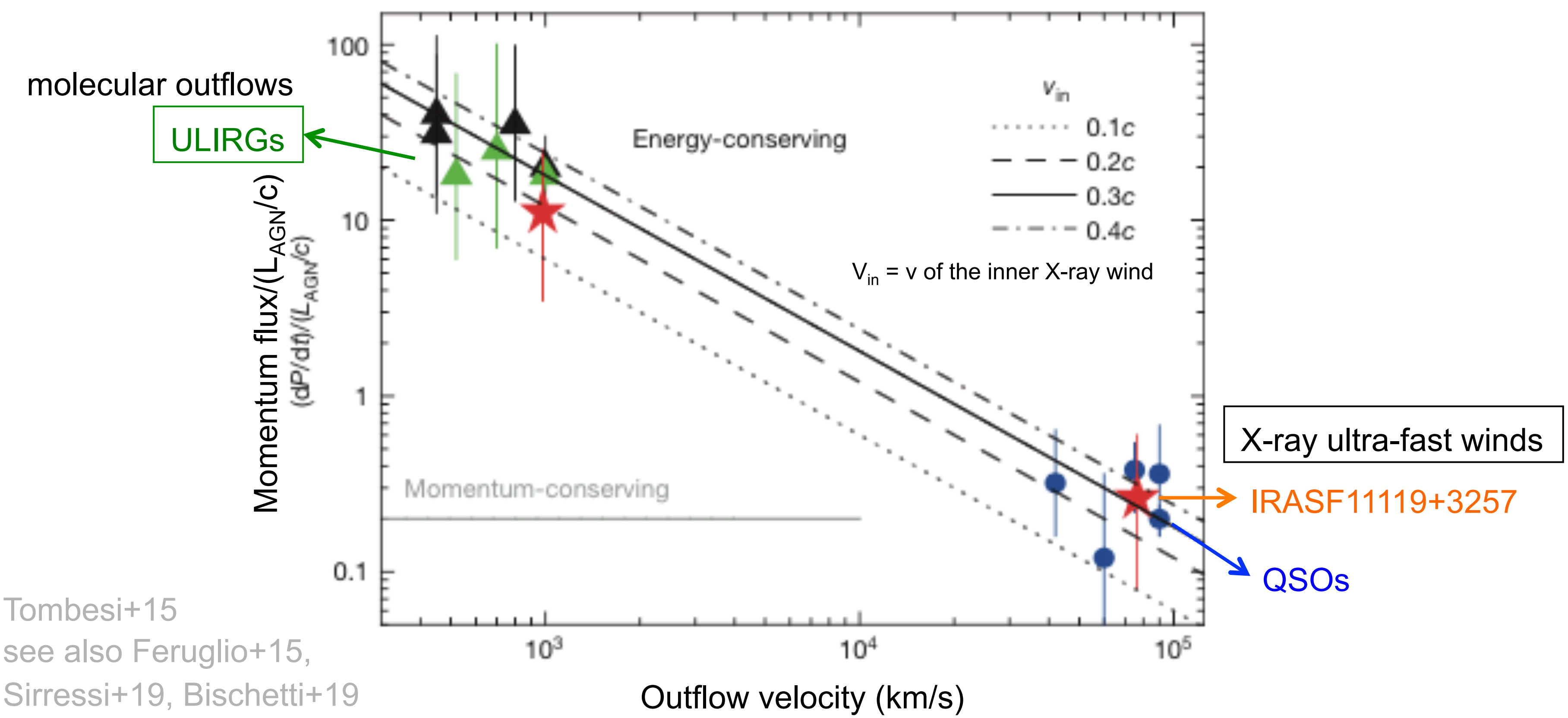

Tombesi+15
see also Feruglio+15,
Sirressi+19, Bischetti+19

UFO detection (v≈0.3c) in IRASF11119+3258 consistent
with energy-conserving outflow from
inner X-rays to outer molecular outflow (Pdot,out ≈12 L_{AGN}/c)

Linking X-ray outflows with molecular outflows. II

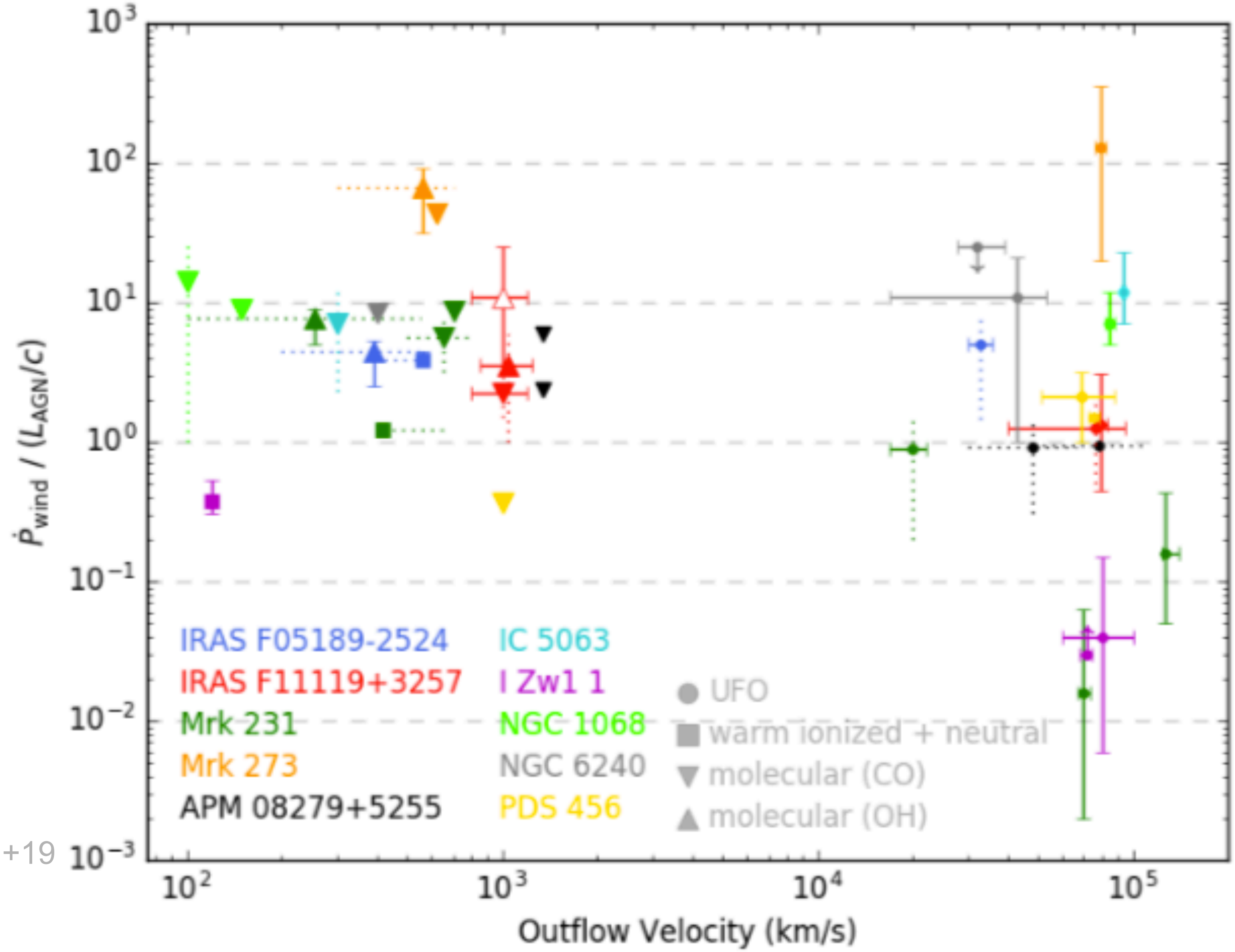

Smith+19